

## Refined scaling hypothesis for breakdown coefficients in turbulence

Remo Badii<sup>1</sup> and Peter Talkner<sup>2</sup><sup>1</sup>*Nortel Networks, HPOCS, Binzstrasse 17, 8045 Zurich, Switzerland*<sup>2</sup>*Paul Scherrer Institute, 5232 Villigen, Switzerland*

(Received 8 February 2001; published 18 June 2001)

We study the statistics of Novikov's breakdown coefficients, which represent ratios between energy dissipation rates at different length scales in turbulence. The distribution of their logarithms is shown to be very closely reproduced by an analytic function that we obtain from a hierarchical stochastic process for the turbulent cascade. Correlations and deviation from Gaussianity in the model are accounted for by two parameters, one of which can be interpreted as a generalized dimension. Finally, we illustrate the lack of power-law scaling in the moments of the breakdown coefficients and propose an analytical approximation scheme for them.

DOI: 10.1103/PhysRevE.64.016307

PACS number(s): 47.27.Gs, 02.50.-r, 05.40.-a

### I. INTRODUCTION

The small-scale structure of turbulent fluids lends itself to a description based on scaling properties of observables measured across spatiotemporal intervals of given lengths. In particular, velocity differences and the rate of dissipation of the kinetic energy are at the core of the fundamental theories of turbulence [1–5].

The moments  $\langle d^p(l) \rangle$  of the longitudinal velocity difference  $d(l) = [\mathbf{v}(\mathbf{x} + \mathbf{l}, t) - \mathbf{v}(\mathbf{x}, t)] \cdot \mathbf{l}/l$ , where  $\mathbf{v}(\mathbf{x}, t)$  is the velocity field of the fluid at the space-time point  $(\mathbf{x}, t)$  and  $\mathbf{l}$  is a displacement vector of length  $l$ , are believed to scale as

$$\langle d^p(l) \rangle \sim l^{\zeta_p} \quad (1.1)$$

in the “inertial range”  $l \in (l_{\min}, l_{\max})$ , with universal exponents  $\zeta_p$  that do not depend linearly on  $p$ .

The energy dissipation rate averaged over a domain of size  $l$  is further defined as

$$\varepsilon(l) = \frac{2\nu}{|B|} \int_B \sum_{ij} S_{ij}(\mathbf{x}) S_{ji}(\mathbf{x}) dV, \quad (1.2)$$

where  $S_{ij} = (\partial v_i / \partial x_j + \partial v_j / \partial x_i) / 2$  is the symmetric part of the strain rate tensor,  $B = B(\mathbf{x}; l)$  is the averaging domain, centered at  $\mathbf{x}$  and having volume  $|B| \sim l^3$ , and  $\nu$  is the kinematic viscosity. In analogy with Eq. (1.1), the moments of  $\varepsilon(l)$  are also expected to exhibit power-law scaling as

$$\langle \varepsilon^p(l) \rangle \sim l^{\tau_p}. \quad (1.3)$$

Furthermore, the exponents  $\zeta_p$  and  $\tau_p$  are believed to satisfy the relation

$$\zeta_p = p/3 + \tau_{p/3} \quad (1.4)$$

that has been obtained within the so-called “refined theory” [2,3] which tries to explain the nonlinearity of  $\zeta_p$  through the fluctuations of  $\varepsilon(l)$ . In such a theory, the energy dissipation rate  $\varepsilon(l)$  is postulated to be log-normally distributed as a result of a cascade process by which  $\varepsilon(l)$  splits itself in a multiplicative, uncorrelated way from large to small eddies in the fluid.

The log-normal model has been shown to be asymptotically incorrect [6] (it yields a quadratic form for  $\tau_p$ , whereas  $\tau_p$  behaves linearly in  $p$  for  $|p| \gg 1$  [11,7]) and several other phenomenological models have been proposed [8–11]. A recent one [12] was shown to be related to log-Poisson statistics [13].

In order to study the cascade process more closely, Novikov [6] introduced ratios  $q = \varepsilon(l') / \varepsilon(l)$  between values of the energy dissipation rate averaged over nested domains of sizes  $l'$  and  $l$ . The moments and the distributions of these quantities, called breakdown coefficients, have been studied in [14,15] as a function of  $r = l'/l$ . A power-law dependence of the moments of  $q(r)$  on  $r$  has been conjectured, in which the exponent may depend on the relative position of the smaller domain within the larger one [15]. The results, however, cast some doubt on this scenario, although the deviations from a power law seem to be smaller here than for the moments (1.3) of  $\varepsilon(l)$ .

Indeed, as we have shown in a previous article [16], the scaling postulated in Eq. (1.3) does not hold and is not expected to hold even for pure self-affine functions of time such as fractional Brownian motion [17]. We reproduced the observed behavior by introducing a refined law, deduced from a stochastic process which accounts for correlations in the calculation of the average (1.2). The result is a ratio of  $\Gamma$  functions that contains two parameters: one of them is akin to a dimension and is closely related to the exponent  $\tau_p$  in a limit in which Eq. (1.3) becomes correct.

In the present work, we apply a similar procedure to a hierarchical description of the cascade and propose a specific analytical form for the distribution of the breakdown coefficients. We further provide evidence for the lack of power-law scaling in  $q(r)$ 's statistics by introducing a sequence of approximating analytic functions for the first moment of the breakdown coefficient. Our analysis yields a remarkable agreement with the experimental results in the whole range  $r \in [0, 1]$ .

We expect our approach to lead to a revised understanding of the “exponent”  $\tau_p$  and of the relations (1.3) and (1.4). Moreover, integration of this form of the distribution of  $q(r)$  into the arguments exposed in [6,14] may lead to more accurate extrapolations for the asymptotic behavior of the mo-

ments  $\langle \varepsilon^p(l) \rangle$  in the limit(s)  $p \rightarrow \infty$  ( $-\infty$ ), although the estimates in [6,14] were obtained within the simple power-law framework.

## II. HIERARCHICAL STOCHASTIC MODEL

Given a scalar time series  $V = \{v_1, v_2, \dots, v_n\}$ , consisting of values of a velocity component in a turbulent fluid, sampled at a fixed position  $\mathbf{x}$  and times  $t_i = i\Delta t$  ( $i = 1, 2, \dots, n$ ), the energy dissipation rate  $E_i(l)$  in the interval  $L_i = [i+1, i+l]$  is usually computed as [18]

$$E_i(l) = \sum_{j=i+1}^{i+l} (v_{j+k} - v_j)^2, \quad (2.1)$$

by neglecting a prefactor that includes the viscosity  $\nu$ , the sampling time  $\Delta t$ , and the shift  $k$ . The average rate in  $L_i$  is then

$$\varepsilon_i(l) = E_i(l)/l. \quad (2.2)$$

The step  $k$  appearing in the velocity difference in Eq. (2.1) controls the evaluation of the gradient and must be adjusted in dependence on  $\Delta t$  [11].

The scaling properties of the energy dissipation field can be studied through the ‘‘breakdown coefficient’’ [6]

$$q_{r,l}(\Delta) = \frac{\varepsilon_i(rl)}{\varepsilon_i(l)}, \quad (2.3)$$

which represents the ratio between two values of the  $\varepsilon$  field computed across nested intervals  $L' \subseteq L$ , of respective lengths  $rl$  and  $l$ , with  $0 \leq r \leq 1$  and  $0 \leq i-j \leq (1-r)l$ . The parameter  $\Delta = (i-j)/[(1-r)l] \in [0,1]$  measures the shift of the inner interval within the outer one. In the following, we shall set  $\Delta = 0$  for simplicity, so that the intervals will have their left extremum in common. Moreover, we shall focus on the overall dissipation rates  $E_i(l)$ , rather than on their locally averaged counterparts  $\varepsilon_i(l)$ , to simplify the notation.

Indicating by  $l' = rl$  the length of the smaller interval  $L'$ , the rate  $E(l')$  can be seen as the result of a cascade of  $n$  fractioning steps across lengths  $l_i$ , with  $l' = l_0 < l_1 < \dots < l_n = l$ , by writing

$$E(l') = E(l) \frac{E(l_{n-1})}{E(l_n)} \frac{E(l_{n-2})}{E(l_{n-1})} \dots \frac{E(l_0)}{E(l_1)}. \quad (2.4)$$

By further setting  $l_i/l_{i+1} = \sigma$ ,  $\forall i$ , and  $r = \sigma^n$ , the (zero-shift) ratio

$$Q(r;l) = E(rl)/E(l) \quad (2.5)$$

can be expressed as

$$Q(r;l) = \prod_{i=1}^n Q(\sigma; l_i) \quad (2.6)$$

or, using the logarithms  $\Lambda(\sigma; l_i) = -\ln Q(\sigma; l_i)$ , as

$$\Lambda(r;l) = -\ln Q(r;l) = \sum_{i=1}^n \Lambda(\sigma; l_i). \quad (2.7)$$

In analogy with Ref. [16], we introduce the probability  $P(\Lambda < \Lambda(r;l) < \Lambda + \Delta\Lambda)$  for  $\Lambda(r;l)$  to fall in the range  $J_\Lambda = (\Lambda, \Lambda + \Delta\Lambda)$  and seek the density

$$\rho_n(\Lambda) = \frac{1}{\Delta\Lambda} P(\Lambda(r;l) \in J_\Lambda), \quad (2.8)$$

which depends on  $r$  and  $l$  through  $\Lambda(r;l)$ : we omit these indices for simplicity. Dividing the interval  $[0, \Lambda]$  into  $N$  subintervals of length  $\Delta\Lambda = \Lambda/N$ , we approximate  $\Lambda(r;l)$  via the sum

$$\Lambda(r;l) = \Delta\Lambda(s_1 + s_2 + \dots + s_n), \quad (2.9)$$

where the symbols  $s_i$  are defined by

$$s_i = \begin{cases} 0 & \text{if } \Lambda(\sigma; l_i) \leq \Delta R \\ 1 & \text{otherwise} \end{cases} \quad (2.10)$$

and  $\Delta R$  is a suitable threshold value which depends on  $N$  and separates the distribution  $P(\Lambda(\sigma; l_i))$  into two parts.

Hence, the value of  $\Lambda(r;l)$  is seen as the position of a one-dimensional random walker at ‘‘time’’  $n$ , for which the step sizes assume two possible values, 0 and  $\Delta\Lambda$ , with probabilities  $p_0$  and  $p_1$ , respectively. The event  $\Lambda(r;l) \in J_\Lambda$  will occur if and only if  $N$  symbols are equal to 1 in  $n$  trials (clearly,  $n \geq N$ ). The probability for this outcome is [19]

$$P(\Lambda(r;l) \in J_\Lambda) = \binom{n-1}{n-N} p_0^{n-N} p_1^N = \frac{n-m}{m} B(m, n; p_0) \quad (2.11)$$

where

$$m = n - N \quad (2.12)$$

is the number of 0 symbols and  $B(m, n; p_0)$  is the binomial distribution for  $m$  successes with probability  $p_0$  in  $n$  trials. The notion of ‘‘success’’ and ‘‘failure’’ is purely arbitrary: here,  $s_i = 0$  is considered a ‘‘success.’’

Furthermore, we approximate  $B(m, n; p_0)$  with the Poisson distribution

$$P(m, \lambda) = \frac{\lambda^m}{m!} e^{-\lambda}, \quad (2.13)$$

for  $n \rightarrow \infty$  and  $p_0 \rightarrow 0$  at constant  $\lambda = np_0$ . Equation (2.10) shows that  $p_0$  is the probability for  $\Lambda(\sigma; l_i)$  to lie in  $[0, \Delta R]$ . As remarked in [16] for generic stochastic processes, the density of  $\Lambda$  and the correlations among the terms in the sum (2.9) may lead to a singular density  $\rho_n(\Lambda)$ , analogous to a ‘‘fractal’’ measure. Therefore, we account for this possibility by introducing a dimensionlike quantity  $D$  and postulating the ‘‘mass-radius’’ scaling relation

$$p_0 \sim a(\Delta R)^D = a \frac{\Lambda^D}{N}, \quad (2.14)$$

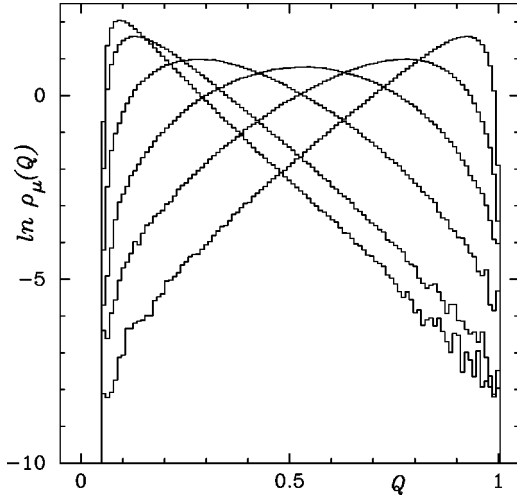


FIG. 1. Histograms of the density  $\rho_\mu(Q)$  vs  $Q$  [Eq. (2.18)] obtained from atmospheric turbulence data for  $r=0.1, 0.15, 0.3, 0.5, 0.7,$  and  $0.85$  (from left to right).

where  $a$  is a proportionality constant. This allows rewriting the parameter  $\lambda$  of the Poisson distribution (2.13) as

$$\lambda = (\Lambda/\Lambda_0)^D, \quad (2.15)$$

where  $\Lambda_0$  is a normalization constant. Collecting all terms, one finally obtains the expression

$$\rho_n(\Lambda) = \frac{D}{\Lambda_0} \frac{(\Lambda/\Lambda_0)^{mD-1}}{\Gamma(m)} e^{-(\Lambda/\Lambda_0)^D}, \quad (2.16)$$

where  $m$  and  $n$  are related through Eq. (2.12). At variance with Ref. [16], where these quantities represented actual steps in the numerical evaluation of  $E(l)$ , here they (as well as  $N$ ) are purely arbitrary parameters. In fact, the fractioning (2.4) is a formal discretization, imposed on a continuous process, which can be carried out with any number of steps. Therefore, we replace  $m$  by a real parameter  $\mu$  in Eq. (2.16) and finally write the desired density as

$$\rho_\mu(\Lambda) = \frac{D}{\Lambda_0} \frac{(\Lambda/\Lambda_0)^{\mu D-1}}{\Gamma(\mu)} e^{-(\Lambda/\Lambda_0)^D}, \quad (2.17)$$

where  $\mu$ ,  $D$ , and  $\Lambda_0$  must be determined from the analysis of the experimental data. Hence,  $\mu$  can be interpreted as the ‘‘depth’’ of the hierarchical cascade which leads from the dissipation rate  $E(l)$  across the length scale  $l$  to its counterpart  $E(l')$  across the length  $l'$  [20].

By changing the variable from  $\Lambda$  to  $Q$  [see Eqs. (2.5) and (2.7)], the distribution is transformed into

$$\rho_\mu(Q) = \frac{D}{\Lambda_0} \frac{[(-\ln Q)/\Lambda_0]^{\mu D-1} e^{-(\ln Q/\Lambda_0)^D}}{\Gamma(\mu) Q}, \quad (2.18)$$

where we have used the same symbol  $\rho$  as in Eq. (2.17), since the presence of the argument ( $Q$  vs  $\Lambda$ ) prevents any ambiguity. In Fig. 1, we show histograms of the density  $\rho_\mu(Q)$ , obtained from atmospheric turbulence data. The lat-

ter consist of wind velocity values, sampled at 3 and 30 kHz, with a Taylor-Reynolds number of about 10 000: a detailed description can be found in [21]. Time series of up to  $10^6$  points have been considered, with  $l \in [300, 600]$  ( $l \in [3000, 6000]$ ) for the 3 (30) kHz data. Notice the symmetry of the curves under the simultaneous transformations  $r \rightarrow (1-r)$ ,  $Q \rightarrow (1-Q)$ . In fact, the interval  $L$  can be written as  $L = L' \cup L''$ , where  $L''$  has length  $(1-r)l$  and  $1-Q = E''/E$ , where  $E'' = E - E'$  is the energy dissipation rate across  $L''$ .

Unfortunately, no general analytical expression is available for the moments

$$M_p(r) = \langle Q^p(r) \rangle \quad (2.19)$$

of  $Q(r)$ . In fact, they are readily seen to be given by the Laplace transform

$$\langle Q^p(r) \rangle = \int_0^\infty e^{-p\Lambda} \rho_\mu(\Lambda; D, \Lambda_0) d\Lambda \quad (2.20)$$

of the density  $\rho_\mu(\Lambda)$  of  $Q$ 's logarithm  $\Lambda$ , for which an analytical expression is available for rational values of  $D$  only (see [22]). Moreover, this involves Meijer's  $G$  functions with arguments too complicated to be profitably used in a fit (and to be reproduced here). In principle, however, the procedure would work as follows. After computing  $M_p(r)$  for a fixed  $p$  and various  $r$  values, one should set  $D = j/k$ , using approximate start values for the integers  $j$  and  $k$ , and estimate  $\mu$  and  $\Lambda_0$  from a fit of the curve  $M_p(r)$ . A few initial values of  $D$  should be tried in order to minimize the error. Then, an iterative procedure which updates  $D$  from successive points in the  $(j, k)$  space could be implemented to further reduce the error.

### III. NUMERICAL RESULTS

The density  $\rho_\mu(Q)$  has been estimated for several sets of experimental data, sampled at both 3 kHz and 30 kHz, using  $l \in [300, 600]$  and  $k \in [3, 8]$ . Although a systematic study of the parameters  $\mu$ ,  $D$ , and  $\Lambda_0$  as functions of  $r$ ,  $l$ , and  $k$  goes beyond the scope of the present article, in this section we present some detailed numerical results.

In Fig. 2, two experimental distributions (corresponding to  $r=0.1$  and  $r=0.6$ , both with  $l=400$  and  $k=5$ ) are compared with fit curves from Eq. (2.18). The agreement is very good, notwithstanding the logarithmic scale, except in the low-probability tail of the most skewed curve ( $r=0.1$ ). Analogous accuracy is obtained at different values of  $r$  and for all values of  $l \in [300, 600]$ . Therefore, one can safely ignore the outer scale  $l$ , as long as it remains in a given range, and consider only the  $r$  dependence of the distributions.

In Figs. 3–5, we display values of  $\mu(r)$ ,  $\ln D(r)$ , and  $\ln \Lambda_0(r)$  versus  $r$ , as obtained from fits performed on  $\rho_\mu(Q)$  (on a linear scale) computed for  $k=5$  and  $l=400$ . Because of the change in the shape of the curves, the fit ranges have been changed from  $Q \in [0, 0.9]$  (for the distribution computed at  $r=0.05$ ), to  $Q \in [0.05, 0.95]$  (for  $r=0.45, 0.5,$  and

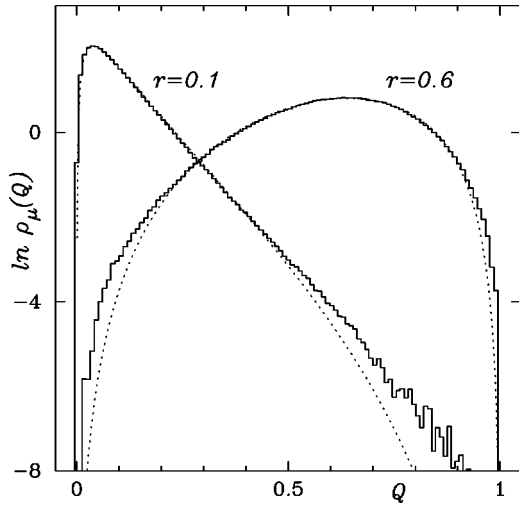


FIG. 2. Plot of  $\ln \rho_\mu(Q)$  vs  $Q$  for  $r=0.1$  and  $r=0.6$  (solid lines), estimated from experimental data, compared with fit curves from Eq. (2.18) (dotted lines). Discrepancies can be seen only in low-probability regions and are hardly discernible in a linear plot.

0.55), to  $Q \in [0.1, 1]$  (for  $r=0.95$ ). Notwithstanding the invariance of the curves under the above-mentioned transformation  $(r, Q) \rightarrow (1-r, 1-Q)$ , no symmetry-invariant expression has been found for the parameters  $\mu$ ,  $D$ , and  $\Lambda_0$ .

As already commented upon, the evaluation of the moments presents more difficulties for  $Q(r)$  than for  $\Lambda(r)$  or for the energy dissipation rate  $\varepsilon(l)$ , which both descend from the distribution of Eq. (2.17) introduced in [16]. In that case, the moments are expressed by the ratio of two  $\Gamma$  functions:

$$\langle \varepsilon^p(l) \rangle \sim \left( \frac{l}{k} \right)^{-p} \frac{\Gamma(\mu_p l/k + p/D_p)}{\Gamma(\mu_p l/k)}, \quad (3.1)$$

where  $\mu_p$  and  $D_p$  are the analog of  $\mu$  and  $D$  in the present work (the index  $p$  showing that they depend on the order of the moments, as discussed in [16]). The connection of the

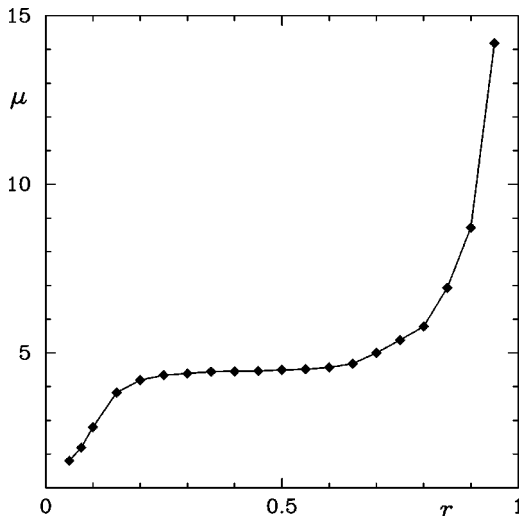


FIG. 3. Plot of the parameter  $\mu$  vs  $r$ , obtained by fitting the distribution in Eq. (2.18) to histograms of experimental data, all computed for  $l=400$  and  $k=5$  [see Eq. (2.1)].

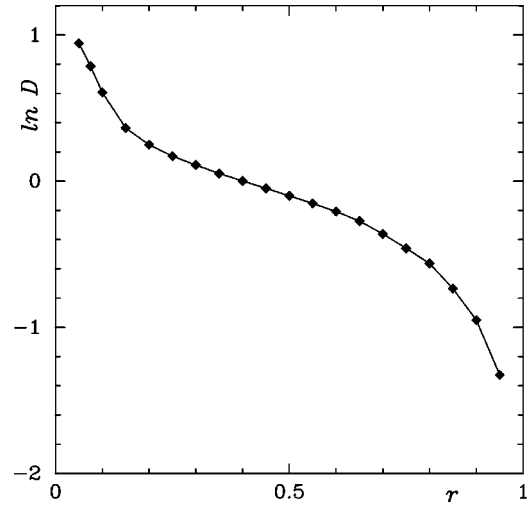


FIG. 4. Same as Fig. 3 for the logarithm of  $D$  vs  $r$ .

refined law (3.1) with the power-law assumption (1.3) was established by noticing that the asymptotic behavior of Eq. (3.1), for  $(\mu_p l)/k \gg p/D_p$ , is

$$\langle \varepsilon^p(l) \rangle \sim l^{-p+p/D_p}, \quad (3.2)$$

which leads to

$$D_p = \frac{p}{p + \tau_p}. \quad (3.3)$$

Hence,  $D_p=1$  is equivalent to  $\tau_p=0$ : this is the case of monoaffine signals. In the present work,  $D$  is primarily studied as a global parameter characterizing the distribution and its  $r$  dependence is singled out, as shown in Fig. 4. It represents a dimensionlike quantity which describes statistical scaling properties of the variable  $\Lambda(r)$ , as discussed in connection with Eq. (2.14).

The values of  $\mu$ , instead, depend on details of the calculations such as, e.g., the time step  $k$  of Eq. (2.1). As shown in [16], it incorporates information about the correlations of the

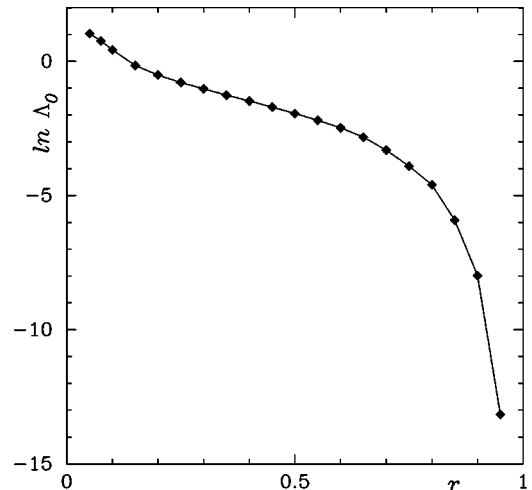


FIG. 5. Same as Figs. 3 and 4 for the logarithm of  $\Lambda_0$  vs  $r$ .

increments in the stochastic process leading to Eq. (2.9). Finally,  $\Lambda_0$  is a normalization constant, with minor physical relevance.

#### IV. RELATIONSHIP WITH TURBULENCE THEORY

In this section, we further elucidate the reason why the moments  $M_p(r)$  [Eq. (2.19)] of the breakdown coefficients  $Q(r)$  cannot be expected to present power-law scaling in  $r$  by introducing an approximation scheme for them which relies on a two-scale analysis of turbulence. We then comment on the relevance of the proposed distribution (2.18) to estimates of the asymptotic behavior of  $\tau_p$  for  $|p| \rightarrow \infty$ .

The dependence of the first moment  $M_1(r) = \langle Q(r) \rangle$  of the breakdown coefficient  $Q(r)$  on  $r$  (again, the  $l$  dependence is considered weak enough to be negligible) can be accurately reproduced by the following procedure. Consider the sequence

$$\{a_0, a_1, a_2, \dots\} = \left\{ \left\langle \frac{E'}{E} \right\rangle, \left\langle \frac{E'}{E} \right\rangle, \left\langle \frac{E'E}{E^2} \right\rangle, \dots \right\}, \quad (4.1)$$

the generic term of which can be written as

$$a_p = \frac{\langle E' E^{p-1} \rangle}{\langle E^p \rangle}, \quad (4.2)$$

where the symbols  $E$  and  $E'$  represent  $E(l)$  and  $E(rl)$ , respectively, as in Eq. (2.5), so that  $\langle Q \rangle = \langle E'/E \rangle = a_0$ . Clearly, the sequence  $A = \{a_0, a_1, a_2, \dots\}$  is monotonic and its terms are bounded within the interval  $[0, 1]$ , for all  $r$ , since  $0 \leq E' \leq E$ . In fact, for  $p \rightarrow \infty$ ,  $a_p$  tends to the average of  $E'$  computed over the set of points (along the time series) at which  $E$  attains its maximum value  $E_{\max}$ , divided by  $E_{\max}$  itself. For  $p \rightarrow -\infty$ , the same occurs, with the minimum  $E_{\min}$  of  $E$  in place of  $E_{\max}$ . By this property, one can construct an iterative scheme to estimate  $a_0(r)$ .

To first order, one might set  $a_0 \approx a_1$ , which just means

$$\langle Q(r) \rangle \sim \frac{\langle E(rl) \rangle}{\langle E(l) \rangle}. \quad (4.3)$$

By further neglecting the more accurate formula (3.1) and reverting to the simpler Eq. (1.3), one would then obtain  $\langle Q(r) \rangle \sim r^{Z_3}$ , where we have indicated with

$$Z_{3p} = p + \tau_p \quad (4.4)$$

the scaling exponents of  $E(l)$  under the power-law assumption

$$\langle E^p(l) \rangle \sim l^{Z_{3p}}. \quad (4.5)$$

Hence, to first order,  $M_1(r)$  varies as a power of  $r$ , as supposed in [9,14,15].

To second order, we set

$$a_0 \approx 2a_1 - a_2 \quad (4.6)$$

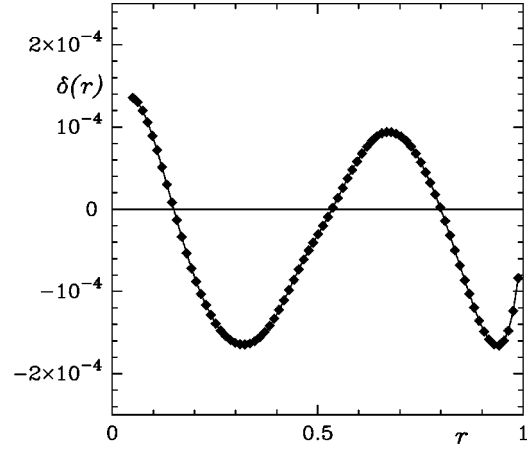


FIG. 6. Difference  $\delta(r)$  between the experimentally evaluated moment  $\langle Q(r) \rangle$  and the approximating (second-order) function  $2r - g(r)$  vs  $r$  of Eq. (4.9), for  $Z_6 = 1.8335$ .

by subtracting the next difference,  $d_1^1 = a_2 - a_1$ , from  $a_1$ , which corresponds to equating the second-order difference  $d_0^2 = d_1^1 - d_0^1$  to zero. The  $k$ th term is therefore obtained from

$$d_0^k = \sum_{j=0}^k (-1)^j \binom{k}{j} a_{k-j} = 0, \quad (4.7)$$

where  $d_0^k(d_n^k)$  is the  $k$ th-order difference computed from  $a_0(a_n)$ .

The crucial point of our scheme lies in the  $r$  dependence of the term  $a_2$  which can be expressed as [21]

$$a_2(r) = \frac{\langle E'E \rangle}{\langle E^2 \rangle} \sim g(r) \equiv \frac{1 + r^{Z_6} - (1-r)^{Z_6}}{2}. \quad (4.8)$$

In the derivation of this result,  $E'E$  is rewritten as  $[E^2 + (E')^2 - (E''^2)]/2$ , where  $E'' = E - E'$  is the energy dissipation rate across the interval  $L''$  of length  $l'' = (1-r)l$  that was defined in Sec. II, and the scaling law (4.5) is used again. Then, since  $Z_3 \approx 1$ , Eqs. (4.6) and (4.8) finally yield

$$a_0(r) = \langle Q(r) \rangle \approx 2r - g(r), \quad (4.9)$$

where the function  $g(r)$  is invariant under the transformation  $(r, g) \rightarrow (1-r, 1-g)$ , has a sigmoidal shape with  $g'(r) \geq 0$ , and satisfies  $g(0) = 0, g(1) = 1$ . Figure 6 illustrates the accuracy of this quite simple approximation which does not even take into account relation (3.1): the difference  $\delta(r)$  between the experimentally evaluated moment  $\langle Q(r) \rangle$  and  $2r - g(r)$  lies in the range  $[-0.0002, 0.00015]$  for  $r \in [0, 1]$ , at the best-fit value  $Z_6 = 1.8335$ .

The third-order approximation requires expressing  $a_3$  as a function of  $r$ . By expanding  $\langle (E - E')^3 \rangle$ , dividing it by  $\langle E^3 \rangle$ , and applying Eq. (4.5), one arrives at

$$\frac{\langle E'E^2 \rangle}{\langle E^3 \rangle} - \frac{\langle E'^2 E \rangle}{\langle E^3 \rangle} \sim \frac{1 - r^{Z_9} - (1-r)^{Z_9}}{3}, \quad (4.10)$$

a relation which is fulfilled to within 0.0002 for  $Z_9 = 2.607$  by our data. This result, however, still leaves us with the task

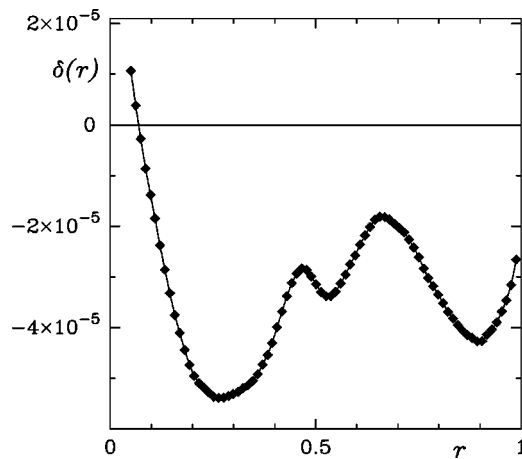


FIG. 7. Same as in Fig. 6 for the third-order approximation (4.11), for  $Z_6 = 1.8345$ .

of expressing the second term on the left-hand side of Eq. (4.10) as a function of  $r$ . Rather than pursuing this difficult goal, we note that the passage from  $a_1(r)$  to  $a_2(r)$  is tantamount to the application of function  $g$  of Eq. (4.8) to  $a_1(r) \approx r$ . This suggests iterating the procedure with the substitution of  $g(g(r))$  for  $a_3(r)$ : that is, pretending that the inclusion of one more factor  $E$  in both numerator and denominator of  $a_p$  has the same effect as the application of the (weakly) nonlinear function  $g$  to the previous term. Deviations from the “true” behavior are thereby accounted for by different values of the parameter  $Z_6$  in  $g(r)$ . In fact, setting

$$a_0(r) \approx 3r - 3g(r) + g(g(r)) \quad (4.11)$$

in our third-order approximation yields an astounding agreement with the experiment, as can be seen in Fig. 7, by choosing  $Z_6 = 1.8345$ : the error is about five times smaller than in Fig. 6. Using higher-order schemes or higher iterates of  $g$  yields no improvement since neither the power-law assumption (4.5) nor the iteration of  $g$  is correct at this level of accuracy.

Extensions of our difference scheme to higher moments are not straightforward because of the difficulty of express-

ing terms of the type  $\langle (E')^q E^p \rangle / \langle E^{q+p} \rangle$  as functions of  $r$  only (i.e., independent of  $l$ ).

Notice that the energy-dissipation-rate exponent  $Z_p$  is assumed to be the same as the velocity-difference exponent  $\zeta_p$  by the ordinary refined theory [2,3], which relies on Eqs. (1.3) and (4.5). Our result for  $Z_6$  would then imply  $\tau_2 \approx -0.166$ , in agreement with our previous estimates [11]. As already remarked, however, the moments of the energy dissipation rate do not scale as power laws: Eqs. (1.3), (1.4), and (4.5) are only rough approximations. This is the reason why we used the symbol  $Z_p$  and not  $\zeta_p$  in Eq. (4.5): the former, in fact, is not rigorously defined by that relation.

As to the relation between our models and classical models in turbulence theory, it should be remarked that our stochastic process leading to the unusual distribution (2.18) is not in direct opposition to the log-normal approach (or to its variants like the log-Poisson model), since it refers to a different quantity, namely, the breakdown coefficient, which is a *ratio* of observables (energy dissipation rates) averaged over nested domains. The usual cascade theories, instead, represent  $\varepsilon(l)$  itself as a product of (infinitely many) contributions, a view which may itself be criticized. On the contrary, no approximation is involved in the factorization we introduce in Eq. (2.4). In addition to this, we account for correlations and deviations from Gaussianity in our derivation.

Finally, Novikov [6] has deduced bounds for  $\tau_p$  under the hypothesis that the moments of  $q(r)$  scale like  $r^{\tau_p}$ : that is, as a power law in  $r$  with the same exponent as for the moments of  $\varepsilon$  and independently of any relative shift  $\Delta$  of the inner and outer intervals. Moreover, he has shown [14] that  $\tau_p/p \rightarrow -1$ , in the limit  $p \rightarrow +\infty$ , if the probability distribution  $\rho(Q)$  has no gap. In the present paper, we have provided an analytic expression for  $\rho(Q)$  which confirms, together with the experimental results, that indeed no gap occurs.

We believe that our refined scaling laws for the moments of  $\varepsilon$  [Eq. (3.1)] and the statistics of  $Q(r)$  [Eq. (2.18)] shed light on the understanding of turbulent cascades and that they provide a solid base for further progress.

- 
- [1] A. N. Kolmogorov, Dokl. Akad. Nauk SSSR **30**, 301 (1941).  
 [2] A. N. Kolmogorov, J. Fluid Mech. **13**, 82 (1962).  
 [3] A. M. Obukhov, J. Fluid Mech. **13**, 77 (1962).  
 [4] U. Frisch, *Turbulence: The Legacy of A. N. Kolmogorov* (Cambridge University Press, Cambridge, 1995).  
 [5] A. S. Monin and A. M. Yaglom, *Statistical Fluid Mechanics*, Vol. 1 (MIT Press, Cambridge, MA, 1971); Vol. 2 (MIT Press, Cambridge, MA, 1975).  
 [6] E. A. Novikov, Appl. Math. Mech. **35**, 321 (1971).  
 [7] R. Badii and P. Talkner, Phys. Rev. E **60**, 4138 (1999).  
 [8] T. Bohr, M. H. Jensen, G. Paladin, and A. Vulpiani, *Dynamical Systems Approach to Turbulence* (Cambridge University Press, Cambridge, 1998).  
 [9] E. A. Novikov, Phys. Fluids A **2**, 814 (1990).  
 [10] C. Meneveau and K. R. Sreenivasan, Phys. Rev. Lett. **59**, 1424 (1987); J. Fluid Mech. **224**, 429 (1991).  
 [11] R. Badii and P. Talkner, Phys. Rev. E **59**, 6715 (1999).  
 [12] Z. S. She and E. L ev eque, Phys. Rev. Lett. **72**, 336 (1994).  
 [13] B. Dubrulle, Phys. Rev. Lett. **73**, 959 (1994).  
 [14] E. A. Novikov, Phys. Rev. E **50**, 3303 (1994).  
 [15] G. Pedrizzetti, E. A. Novikov, and A. A. Praskovskiy, Phys. Rev. E **53**, 475 (1996).  
 [16] R. Badii and P. Talkner, Physica A **291**, 229 (2001).  
 [17] B. B. Mandelbrot and J. W. Van Ness, SIAM Rev. **10**, 422 (1968).  
 [18] Temporal displacements at a fixed position are equivalent to spatial displacements at a fixed time by Taylor’s hypothesis: see G. I. Taylor, Proc. R. Soc. London, Ser. A **164**, 476 (1938).

Therefore, the symbol  $l$  will denote temporal displacements in the discussion of the data analysis.

- [19] W. Feller, *An Introduction to Probability Theory and Its Applications*, 3rd ed., Vol. 1 (Wiley, New York, 1968).
- [20] Actually,  $m$  is a nondecreasing function of the equally arbitrary parameter  $N$ , which measures the size of the increments  $\Delta\Lambda$ .

Hence,  $\mu$  represents the depth of the process with respect to the resolution  $N$ .

- [21] R. Badii and P. Talkner, *Europhys. Lett.* **43**, 284 (1998).
- [22] A. P. Prudnikov, Yu.A. Brychkov, and O. I. Marichev, *Direct Laplace Transforms* (Gordon and Breach, New York, 1992), p. 31.